Research Article | Vol. 27, No. 6 | 18 Mar 2019 | OPTICS EXPRESS 8081
Optics EXPRESS

Mode coupling by scattering in chiral nematic liquid crystal ring lasing

KRISTIAAN NEYTS,[1,2,*] TIGRAN DADALYAN,[3] FREDERIK VAN ACKER,[1,2] INGE NYS,[1,2] AND JEROEN BEECKMAN[1,2]

[1]LCP Group, ELIS Department, Ghent University, Technologiepark Zwijnaarde 15, 9052 Gent, Belgium
[2]Center for Nano and Bio Photonics, Ghent University, Technologiepark Zwijnaarde 15, 9052 Gent, Belgium
[3]Yerevan State University, 1 Alex Manoogian, Yerevan 0025, Armenia
[*]kristiaan.neyts@ugent.be

Abstract: Lasing in dye-doped chiral nematic liquid crystal can be realized with low pump energy and relatively high efficiency, thanks to the high reflectivity of the periodic structure. When the helical axis is oriented perpendicular to the substrates, the main lasing peak is normal to the substrates. In some cases, ring lasing of a particular wavelength is observed into an emission cone with axial symmetry. In this paper we explain how scattering of light in the liquid crystal layer leads to optical coupling between normal modes and inclined modes. Based on a numerical model that takes into account spontaneous emission, gain and scattering we show that scattering leads to emission characteristics that are similar to experimental results.

1. Introduction

A chiral liquid crystal (CLC) introduced between two parallel substrates can spontaneously form a helical structure with its axis perpendicular to the substrates. The resulting periodic structure strongly interacts with light if the pitch of the helix is similar to the wavelength of the light. The most striking effect is that circularly polarized light with the same handedness as the CLC is effectively reflected by a CLC layer, if the wavelength lies within an interval called the photonic band gap of the CLC. For this interval the CLC acts like a mirror, but with different properties than a metallic mirror: only circularly polarized light is (completely) reflected and the handedness of the reflected light is the same as that of the incident light. The mirror property of the CLC can be used to make a laser when the CLC is doped with fluorescent dye molecules.

CLC lasing from layers with the helical axis perpendicular to the substrates has been investigated by many groups. It has been observed that lasing often occurs in the direction perpendicular to the substrates for wavelengths near the short-wavelength edge (SWE) or long-wavelength edge (LWE) of the photonic band gap [1–7]. In addition to lasing in the perpendicular direction, there have been observations of lasing for different inclination angles θ (the angle with the helical axis in air). This type of lasing is called color cone lasing and was investigated by Lee and associates [8–10]. The emission wavelength in the color cone lasing is blue shifted for increasing inclination angle, corresponding to the blue shift of the LWE with the inclination angle. Laser light that is trapped inside the CLC layer may also appear in leaky modes in the glass, for inclination angles close to 90° as investigated by Palto et al. [11].

Lasing is a non-linear phenomenon and occurs only when the excitation level, usually by pumping with a pulsed laser, is sufficiently strong. Also at excitation levels well below the lasing threshold, the structure of the CLC has an important influence on the fluorescent spectrum. This is because the structure acts as a one-dimensional microcavity and directly emitted waves interfere with reflected waves. The fluorescent emission from dye molecules

#349097 https://doi.org/10.1364/OE.27.008081
Journal © 2019 Received 25 Oct 2018; revised 1 Dec 2018; accepted 4 Dec 2018; published 5 Mar 2019

Optics EXPRESS

inside a CLC structure, including the wavelength and inclination dependency, is well understood [12,13]. Lasing is obtained by adding gain to the liquid crystal medium until the emission for one particular angle and one particular wavelength diverges [11,14].

The aim of this paper is to explain the occurrence of a lasing ring, with wavelength λ* (equal to the SWE for normal emission) and inclination angle θ* (equal to the angle where the LWE has shifted to the wavelength λ*). The fact that often a bright ring is observed at a particular angle has been reported by Lee and associates [8–10,15]. Fluorescent emission spectra (below the lasing threshold) and lasing spectra have been measured for different devices and different emission angles. The experimental results are discussed and the authors mention that there must be some kind of coupling between the normal lasing spot and the bright laser ring.

In this work we present new experimental results in which the emission spectra above and below lasing threshold are shown as a function of the emission angle. In addition, we explain the observed results by introducing a numerical model that takes into account scattering in the liquid crystal layer. Scattered light contributes to the source term of the emission and this leads to a coupling between the normal SWE mode and the LWE mode that is shifted to the same wavelength for a certain inclination angle.

2. Materials and methods

A liquid crystal device filled with dye-doped CLC has been fabricated in the clean room of UGent. The glass substrates of the LC cell are coated with Nylon 6/6 (Sigma Aldrich) and rubbed in anti-parallel direction in order to obtain planar alignment. The LC cell has an area of 10x10 mm^2 and the cell thickness is about 10 µm. We have used a mixture of the commercially available nematic LC E7 (Merck), with 5 wt% chiral dopant BDH1305 (Licristal, Merck) and 1 wt% of the Pyrromethene dye PM597 (Exciton). The PM597 dye has a maximum in the absorption spectrum around 530 nm and a maximum in the fluorescence spectrum around 590 nm. The dye-doped CLC mixture was heated above the isotropic phase transition temperature and capillary filled into the LC cell. Then the LC cell was slowly cooled to room temperature where it forms a CLC with the helical axis perpendicular to the plane of the substrates. The pitch *P* of the CLC is about 366 nm. The reflection spectrum of the cell is shown in Fig. 1(a). A few disclination lines could be observed in the cell, but all the measurements were made in a homogenous region with the same pitch.

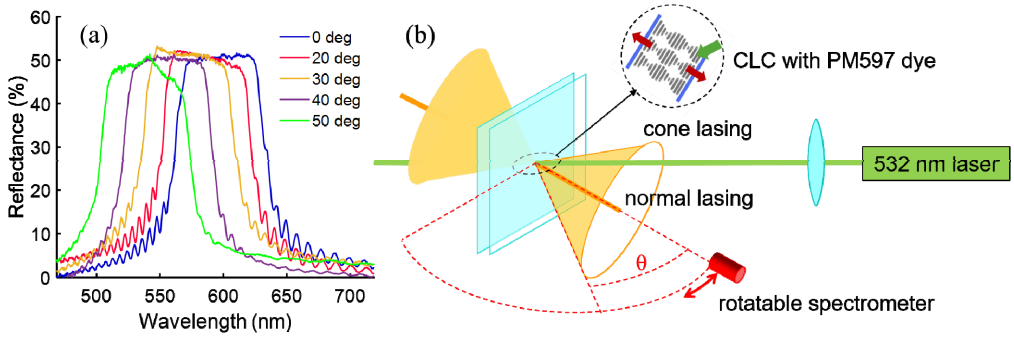

Fig. 1. (a) Reflection spectra of the CLC cell, showing a blue shift of the reflection band for increasing angles of incidence (measured in air). (b) Setup for the measurement of the angle- and wavelength- dependency of emission and lasing from a dye-doped CLC cell that is excited by a pulsed laser (532 nm). The inset illustrates the orientation of the CLC helical axis (only one of the 26 pitches is shown). A spectrometer measures the emission spectrum as a function of the angle θ.

The experimental setup to measure the emission is shown in Fig. 1(b). For optical pumping of the dye-doped CLC cell we use a 532 nm wavelength laser (frequency-doubled pulsed Nd:YAG, Powerchip PNG-M02010, Teem Photonics) that generates 300 ps pulses at a

Optics EXPRESS

repetition rate of 10 Hz to excite the sample. The optical power of the pump beam is controlled by means of a half-wave plate and a polarizing beam splitter (not shown in Fig. 1(b)). The pump beam is focused on the LC cell by means of a lens with 75 mm focal length. The position of the focusing lens is controlled by means of a micrometer stage which enables to adjust the diameter of the pump beam on the LC cell. The FWHM diameter of the pump beam varies between 8 and 11 μm. The LC cell has its normal inclined over 45° with respect to the pump beam in order to separate the pump beam from the emitting laser light. The light emission and lasing is captured by means of a 50 μm diameter core optical fiber, that is positioned on a rotating stage and directed towards the excited spot on the LC cell. This allows to collect light emitted by the dye-doped CLC cell as a function of the inclination angle θ. Emission spectra for different angles are measured with a Q-wave spectrometer with a resolution of 0.5 nm. To improve the dynamic range and avoid saturation, measurements taken with different neutral density filters are scaled and combined into a single intensity graph.

3. Experimental

The results of the measurements are shown in Fig. 2 for three different pump intensities. The pump energy per laser pulse was about 7 μJ. The energy density on the CLC substrate is varied by changing the diameter of the illuminated spot, which is realized by moving a lens. The diameter of the spot is varied between 8 and 11 μm, which means that the area of the spot (and the maximum intensity) varies by about a factor two. The maximum intensity in the center of the spot was about 10^4 J/m^2. The figures show the intensity of the emission by a color code as a function of the wavelength (horizontal axis) and emission angle in air (vertical axis). The band gap of the CLC in the perpendicular direction (θ = 0°) is between 567 nm (SWE) and 636 nm (LWE). Both band edges shift to shorter wavelengths for larger inclination angles. The wavelength dependency on the emission angle measured in air is approximately given by:

$$\lambda_{SWE}(\theta_{air}) = n_o P\sqrt{1-\frac{\sin^2(\theta_{air})}{n_o^2}} \qquad \lambda_{LWE}(\theta_{air}) = n_e P\sqrt{1-\frac{\sin^2(\theta_{air})}{n_e^2}} \quad (1)$$

Figure 2(a) shows a higher intensity of the emission spectrum around 590 nm for all emission angles. This corresponds to the emission maximum of the PM597 dye. We ascribe this contribution to spontaneous emission of the dye. The angle dependency of the LWE is visible as a line of higher intensity with decreasing angle as a function of the wavelength. For emission angles outside of the band gap region (θ>40°) the intensity is higher, as expected, because both left-handed and right-handed polarized light can be emitted. There is a noisy background in this measurement because the signal of spontaneous emission is rather small. The angle dependencies for the SWE and LWE given in Eq. (1), using n_o = 1.55, n_e = 1.74 and P = 366 nm are indicated by a black dashed line, which serves as a guide to the eye (dispersion has not been included).

Figure 2(b) shows a strong peak at n_oP = 567 nm for θ = 0°, which corresponds to the SWE emission of the CLC cavity. The intensity of this peak depends strongly on the energy density of the pump beam and therefore this peak is ascribed to lasing. The emission band around 590 nm is still observed but its relative intensity is smaller.

Finally, in Fig. 2(c) (at the highest excitation density) there are several lasing peaks: at 0° for both the SWE (567 nm) and LWE (636 nm); a third peak is observed at the same wavelength of the SWE in the normal direction (567 nm) but at an emission angle of 54°. The third peak has been studied previously and is often referred to as ring lasing [9].

Finally, there is a range of angles and wavelengths along the LWE line where amplified spontaneous emission is observed and the intensity is higher. Others have found that such emission may reach the threshold for lasing, leading to the name color cone lasing [8], with

Optics EXPRESS

different wavelengths emitted in different cone angles. Figure 2(c) also reveals vertical lines of high intensity, in particular for the wavelengths corresponding to SWE and LWE lasing in the perpendicular direction. All measurements have a background intensity of about 10^{-9} in arbitrary units.

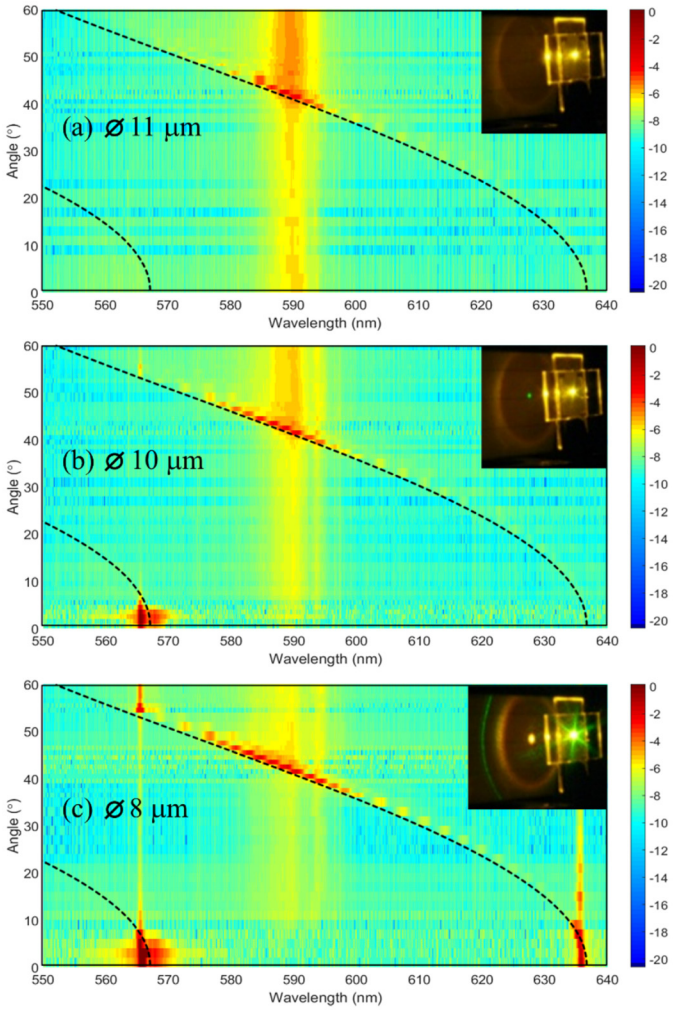

Fig. 2. Measured emission as a function of wavelength and emission angle θ in air for the same dye-doped CLC device at different excitation levels. (a) low excitation level (11 µm beam diameter); (b) medium excitation level (10 µm beam diameter); (c) high excitation level (8 µm beam diameter). The color scale (in nW/nm on the spectrophotometer) is logarithmic. The dashed lines indicate the angle dependency according to Eq. (1). The inset shows a picture of the excited cell and the projection of the emission on a screen.

4. Theoretical model

In this section we describe a theoretical model for fluorescent emission and emission with gain, that is based on CLC doped with dye molecules that are excited by a pump beam. In addition to previous work, we investigate the effect of scattering in the liquid crystal. A layer CLC with positive anisotropy ($n_e > n_o$) and pitch p (right-handed) is placed between two parallel glass plates (normal along the z-axis and refractive index n_g), separated by a thickness d (interfaces at $z = -d/2$ and $d/2$). We assume that the director remains parallel with the glass plates and that d is a multiple of $2p$. In this case the director is for example given by

Optics EXPRESS

$\cos(2\pi z/p)\mathbf{1}_x + \sin(2\pi z/p)\mathbf{1}_y$ which is along the *x*-axis in the center (z = 0) and at the interfaces. The dye material is excited by a pump laser, and we assume that the excitation level is independent of the z-coordinate. The excitation leads to the presence of gain in the medium. The gain for fields parallel and orthogonal to the director depends on the order parameter of the dye molecules and the anisotropy of the dipole transition. We describe gain by attributing a complex part to the refractive indices: $n_e^c = n_e + jg_e$ and $n_o^c = n_o + jg_o$, with the values for *g* typically smaller than the refractive indices.

Following the approach of the scattering matrix introduced by Ko [16], and Penninck [17] we consider plane waves with propagation vector in the *xz*-plane and fields independent of the *y*-coordinate, that propagate in the anisotropic medium. The periodicity along the *x*-axis is determined by the projection κ of the wave vector on the *x*-axis, which is independent of the medium due to Snell's law, and equal to 2π.sinθ/λ in air. In a plane with given coordinate *z*, the director is independent of *x* and *y* and the field eigenmodes for light propagation in the uniaxial material are given by:

$$\mathbf{E}_{o/e,\pm} \exp\left(j\omega t - j\kappa x \mp jk_{z,o/e} z\right) \tag{2}$$

with the upper/lower sign corresponding to propagation in the direction of increasing/decreasing z and o/e indicating the two polarizations (ordinary, with refractive index n_o and extra-ordinary with refractive index n_{eff}). The projection of the wave vector on the z axis depends on κ and on the director of the liquid crystal:

$$\begin{aligned} k_{z,o}^2 &= \left(\frac{2\pi}{\lambda}\right)^2 n_o^{c2} - \kappa^2 \\ k_{z,e}^2 &= \left(\frac{2\pi}{\lambda}\right)^2 n_e^{c2} - \left(1 - \frac{n_o^{c2}}{n_e^{c2}}\right)\cos^2\frac{2\pi z}{p}\kappa^2 - \kappa^2 \end{aligned} \tag{3}$$

Here we are dealing with CLC with an inhomogeneous director, and a 4 by 4 matrix method is needed to describe propagation and reflection from slab to slab, with each slab having a different director. This method has been treated in other papers [3,13] and can be used to simulate the reflection for light incident from *z* = 0 onto the CLC layer with thickness *d*/2. The director in the plane *z* = 0 is chosen along *x*, the fields for the ordinary waves are parallel to the *y*-axis and the fields for the extra-ordinary waves are lying in the *xz*-plane. The reflected o and e waves (travelling in the -*z* direction) are related to incident o and e waves (travelling in the + *z* direction) that have the same parameter κ:

$$\begin{bmatrix} E_{r,o,-} \\ E_{r,e,-} \end{bmatrix} = \begin{bmatrix} r_{oo} & r_{oe} \\ r_{eo} & r_{ee} \end{bmatrix} \begin{bmatrix} E_{i,o,+} \\ E_{i,e,+} \end{bmatrix} \text{ and } \begin{bmatrix} E_{r,o,+} \\ E_{r,e,+} \end{bmatrix} = \begin{bmatrix} r_{oo} & -r_{oe} \\ -r_{eo} & r_{ee} \end{bmatrix} \begin{bmatrix} E_{i,o,-} \\ E_{i,e,-} \end{bmatrix} \tag{4}$$

in which the *r* values are complex reflection coefficients that depend on the parameters of the structure and on κ. The relation between the two reflection matrices arises from the fact that the o-axis in *z* = 0 is a two-fold rotation axis for the CLC structure.

Let us consider now all contributions to plane waves at *z* = + ε travelling in the + *z* direction, due to the light emission of a dye molecule in the center of the CLC layer (*z* = 0). The incident waves $E_{i,o/e,\pm}$ may be reflected and multiple coherent reflections lead to the following equation for the total amplitudes $E_{tot,o/e,+}$:

$$\begin{bmatrix} E_{tot,o,+} \\ E_{tot,e,+} \end{bmatrix} = \begin{bmatrix} E_{i,o,+} \\ E_{i,e,+} \end{bmatrix} + \begin{bmatrix} r_{oo} & -r_{oe} \\ -r_{eo} & r_{ee} \end{bmatrix} \begin{bmatrix} E_{i,o,-} \\ E_{i,e,-} \end{bmatrix} + \begin{bmatrix} r_{oo} & -r_{oe} \\ -r_{eo} & r_{ee} \end{bmatrix} \begin{bmatrix} r_{oo} & r_{oe} \\ r_{eo} & r_{ee} \end{bmatrix} \begin{bmatrix} E_{tot,o,+} \\ E_{tot,e,+} \end{bmatrix} \tag{5}$$

The total amplitudes can be found by solving the following set of two (complex) linear equations:

Optics EXPRESS

$$\left(\begin{bmatrix}1 & 0\\ 0 & 1\end{bmatrix}-\begin{bmatrix}r_{oo} & -r_{oe}\\ -r_{eo} & r_{ee}\end{bmatrix}\begin{bmatrix}r_{oo} & r_{oe}\\ r_{eo} & r_{ee}\end{bmatrix}\right)\begin{bmatrix}E_{tot,o,+}\\ E_{tot,e,+}\end{bmatrix}=\begin{bmatrix}E_{i,o,+}\\ E_{i,e,+}\end{bmatrix}+\begin{bmatrix}r_{oo} & -r_{oe}\\ -r_{eo} & r_{ee}\end{bmatrix}\begin{bmatrix}E_{i,o,-}\\ E_{i,e,-}\end{bmatrix} \quad (6)$$

The coefficient matrix on the left-hand side describes the feed-back mechanism due to multiple reflections. The product of the two reflection matrices can be diagonalized. The (complex) eigenvalues indicate the amplification and phase delay after two reflections, the (complex) eigenvectors indicate the Jones vectors (or the polarization vectors) of the light (eigenmodes) that remain unchanged after reflection. The diagonalization is written with the following notation:

$$\begin{bmatrix}r_{oo} & -r_{oe}\\ -r_{eo} & r_{ee}\end{bmatrix}\begin{bmatrix}r_{oo} & r_{oe}\\ r_{eo} & r_{ee}\end{bmatrix}=\begin{bmatrix}J_{1o} & J_{2o}\\ J_{1e} & J_{2e}\end{bmatrix}\begin{bmatrix}\mu_1 & 0\\ 0 & \mu_2\end{bmatrix}\begin{bmatrix}J_{1o} & J_{2o}\\ J_{1e} & J_{2e}\end{bmatrix}^{-1} \quad (7)$$

The eigenvectors J_1 and J_2 shown in the two columns of the first matrix are the Jones vectors of the polarization states that remain unchanged after two consecutive reflections. The complex eigenvalues μ_1 and μ_2 indicate the amplitude and phase after two reflections. The values of $|\mu_1|$ and $|\mu_2|$ depend on the wavelength λ and on κ (and thus on θ), and below the lasing threshold, they remain below unity.

After substitution of the product of the reflection matrices, we find the solution for the total fields:

$$\begin{bmatrix}1-\mu_1 & 0\\ 0 & 1-\mu_2\end{bmatrix}\begin{bmatrix}J_{1o} & J_{2o}\\ J_{1e} & J_{2e}\end{bmatrix}^{-1}\begin{bmatrix}E_{tot,o,+}\\ E_{tot,e,+}\end{bmatrix}=\begin{bmatrix}J_{1o} & J_{2o}\\ J_{1e} & J_{2e}\end{bmatrix}^{-1}\left(\begin{bmatrix}E_{i,o,+}\\ E_{i,e,+}\end{bmatrix}+\begin{bmatrix}r_{oo} & -r_{oe}\\ -r_{eo} & r_{ee}\end{bmatrix}\begin{bmatrix}E_{i,o,-}\\ E_{i,e,-}\end{bmatrix}\right) \quad (8)$$

This equation illustrates that the total field diverges when one of the eigenvalues becomes equal to one, because matrix inversion becomes impossible. Instead of the decomposition in e- and o-fields, we may also use a decomposition in the eigenvectors J1 and J2 introduced above. In this case we rewrite the above equation in the following form:

$$\begin{bmatrix}1-\mu_1 & 0\\ 0 & 1-\mu_2\end{bmatrix}\begin{bmatrix}E_{tot,1,+}\\ E_{tot,2,+}\end{bmatrix}=\begin{bmatrix}E_{i,1,+}\\ E_{i,2,+}\end{bmatrix} \quad (9)$$

Below the threshold for lasing, the intensity and the polarization of the transmitted emission in the glass substrate in the + z direction is found by multiplication with the transmission matrix (a similar formula can be found for the –z direction):

$$\begin{bmatrix}E_{t,o,+}\\ E_{t,e,+}\end{bmatrix}=\begin{bmatrix}t_{oo} & t_{oe}\\ t_{eo} & t_{ee}\end{bmatrix}\cdot\begin{bmatrix}E_{tot,o,+}\\ E_{tot,e,+}\end{bmatrix} \quad (10)$$

Now we introduce scattering into the model. It is well known the fluctuations in the director orientation in a nematic or chiral nematic liquid crystal lead to scattering of light [8]. Scattering is introduced in the model by coupling between waves $E_{\text{tot},+}$ with the same wavelength, but different directions of propagation (different inclination θ and azimuth φ as illustrated in Fig. 1) at the location $z = 0 +$. Typically there are many simultaneous contributions to scattering, also from different locations x,y,z. All these scattered contributions may have different phases, and therefore we treat them as incoherent. This means that we will couple the powers (and not the fields) of modes with different values of the inclination angles θ (and different values of κ). The flux of radiation per unit area at $z = 0$ is obtained from the electric field by calculating the Poynting vector. Note that the Poynting vector is proportional with the square of the electric field:

$$\mathbf{S}=\frac{1}{2\omega\mu}\mathrm{Re}\left(\mathbf{E}\times\left(\mathbf{k}^{*}\times\mathbf{E}^{*}\right)\right) \quad (11)$$

Optics EXPRESS

with μ in this formula (not the eigenvalue but) the magnetic permittivity. In this work we assume isotropic scattering, which means that the fluxes into different emission directions (in this section, the angle θ refers to the glass substrate) contribute in the same way to scattering. The following scattering equation for fluxes at z = 0 indicates that scattered light (the integral) is added incoherently to the incident flux $S_{i,m,+}$ in the central layer:

$$\left|1-\mu_m(\theta)\right|^2 S_{tot,m,+}(\theta) = S_{i,m,+}(\theta) + c_{scat}\int_0^{\theta'_{max}} \left(S_{tot,1,+}(\theta') + S_{tot,2,+}(\theta')\right) 2\pi \sin\theta' d\theta' \quad (12)$$

In this equation *m* is the eigenmode number for a particular inclination angle (equal to 1 or 2, for the eigenmodes J_1 or J_2), $S_{i,m,+}$ is the flux associated with the field $E_{i,m,+}$ and c_{scat} is a constant indicating the probability for scattering. The above equation reduces to a set of linear equations when the continuous integration is replaced by a sum over equally spaced intervals Δθ:

$$\left|1-\mu_m(\theta_i)\right|^2 S_{tot,m,+}(\theta_i) = S_{i,m,+}(\theta_i) + c_{scat}\sum_j\sum_n S_{tot,n,+}(\theta_j) 2\pi \sin\theta_j \Delta\theta \quad (13)$$

When the incident fluxes $S_{i,m,+}$ are known, this set of equation can be solved for $S_{tot,m,+}$ by simple inversion of a coefficient matrix. When the determinant of the coefficient matrix becomes zero, the threshold for lasing is reached and $S_{tot,m,+}$ can be different from zero, even if all $S_{i,m,+}$ are zero.

To find the fluxes in air, we use the following procedure. From the flux (or Poynting vector amplitude) $S_{tot,m,+}$ of the known eigenmode m + in the central layer, we determine the associated field $E_{tot,m,+}$. This field is then decomposed into its o- an e-components ($E_{tot,o,+}$ and $E_{tot,e,+}$) and the transmitted fields in air are obtained from Eq. (10).

We now examine the example of having two modes A and B with given angles and polarizations, that have values $\left|\mu_1(\theta_A)\right|$, $\left|\mu_2(\theta_B)\right|$ which are much higher than for the other modes. For this case the coefficient matrix has only two rows for which the term in c_{scat} is important. Coupled lasing between the two modes is obtained when the determinant in the coefficient matrix is zero:

$$\begin{vmatrix} \left|1-\mu_1(\theta_A)\right|^2 - c_{scat}\, 2\pi \sin\theta_A \Delta\theta & -c_{scat}\, 2\pi \sin\theta_B \Delta\theta \\ -c_{scat}\, 2\pi \sin\theta_A \Delta\theta & \left|1-\mu_2(\theta_B)\right|^2 - c_{scat}\, 2\pi \sin\theta_B \Delta\theta \end{vmatrix} = 0 \quad (14)$$

The condition for coupled lasing may be reached, if both eigenvalues μ are smaller than unity (and the individual modes do not reach the condition for lasing) and c_{scat} is sufficiently large. The resulting emission will have contributions in both modes $S_1(\theta_A)$ and $S_2(\theta_B)$, with the same wavelength.

In the above approach, we condensed scattering effects into the central layer of the chiral liquid crystal. Scattering may also be present in the outer layers (close to one of the substrates). The result of this type of scattering is that some light (with the same wavelength as the lasing mode) may be emitted in all directions, even in directions that correspond to the optical band gap.

5. Numerical simulations

To illustrate the theoretical model, the emission has been numerically calculated for a particular example. The pitch of the CLC is 367 nm and the thickness *d* of the cell is 3.67 μm, which corresponds to 10 pitches. The director at the surfaces and in the center are chosen along the x-axis. The thickness used in the simulations is (about 3 times) thinner than for the experimental device, because otherwise the emission modes become very narrow and the

Optics EXPRESS

resolution in wavelength and angle has to be increased a lot to avoid discontinuities in the results. We found that using a device with only 10 pitches, makes it possible to illustrate mode coupling very well. For the refractive indices of the liquid crystal E7 and glass, we included the wavelength dispersion [18]. The simulation program, based on the equations given in the previous section, provides the emission into glass. The emission into air is obtained by assuming refraction according to the law of Snell.

Figure 3 shows the amplitude and phase of the factor μ for the mode with the largest absolute eigenvalue as a function of the emission wavelength and the angle in air. In the band gap the amplitude of the eigenvalue is large (strong reflection). Near the SWE the phase of the μ becomes 0° while near the LWE the phase of μ becomes 360°.

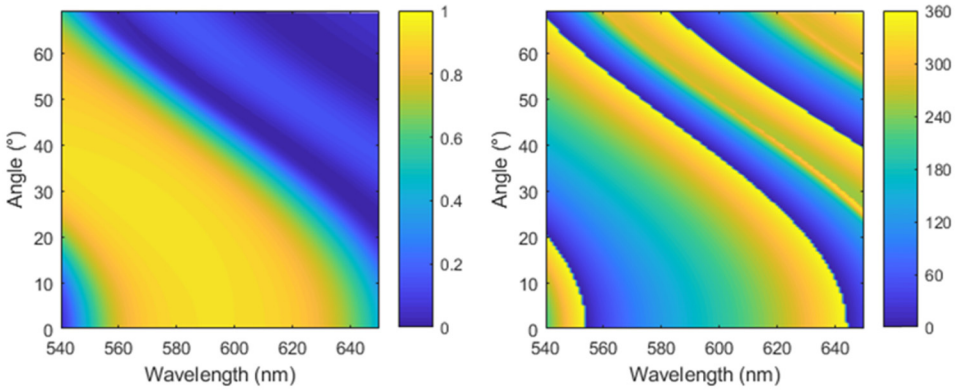

Fig. 3. Amplitude (left) and phase (right, in degrees) of the complex eigenvalue μ with the largest amplitude, as a function of the wavelength λ (horizontal axis) and the emission angle in air θ (vertical axis).

For the spontaneous emission, we assume that it originates at z = 0; that the dye has a white spectrum and that its long axis is orientated parallel to the *xy*-plane, making an angle of 30° with the x-axis. As a result, there is spontaneous emission in both the LWE and SWE. In the simulations we work with a gain in the liquid crystal of 0.155 μm^{-1}, corresponding to $g_e = g_o = 0.155\ \mu m^{-1} \times \lambda/4\pi$. Note the value that we use here is high enough to visualize the effect of amplification, but small enough to remain below the condition for lasing. Therefore, we can use the model discussed above.

Figure 4 shows the emission in air as a function of the wavelength and the inclination angle θ in air for four different cases: without gain or scattering, with gain (no scattering), with scattering (no gain) and with both gain and scattering. For the case without gain and scattering, we obtain the known result that the most intense emission appears near the short and long wavelength edges. Outside of the band gap, for larger angles, there are two weaker modes. In the simulation with gain the highest intensities are further enhanced, leading to an increase in contrast.

For the simulations with scattering, we use the value 0.005 for the scattering coefficient *c*, which means that 0.5% of the intensity that enters the z = 0 plane is scattered into random directions. In literature, we find scattering coefficients β (inverse of the scattering length) in the order of 0.03 μm^{-1} for chiral liquid crystal devices [3,19] which means that our choice for *c* is reasonable for a device with thickness 3.67 μm.

The result is that the intensity is enhanced for wavelengths below $\lambda_{LWE}(0°)$ and also for wavelengths below $\lambda_{SWE}(0°)$, because scattering of emission near the edge of the band gap contributes to the emission in other directions. Finally, in the simulation with gain and scattering, the coupling between the SWE and LWE leads to an enhanced emission of the LWE mode at inclination angle of 58° for the wavelength of 556 nm, which corresponds to the SWE emission at 0°.

Optics EXPRESS

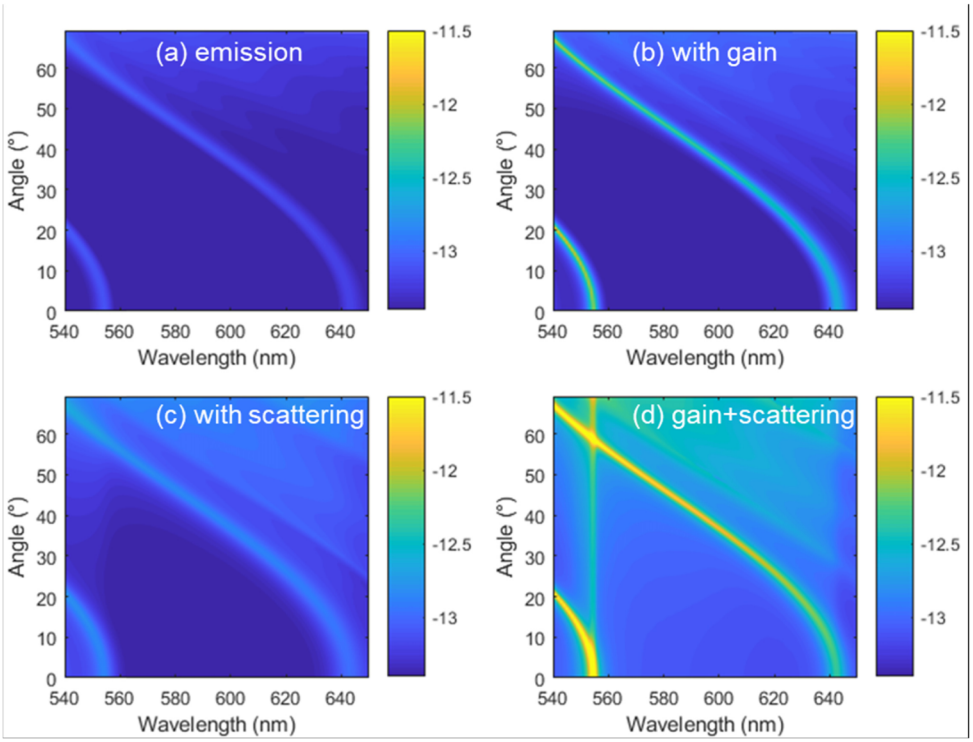

Fig. 4. Simulated emission ($\log_{10}$ color scale) for dye-doped CLC as a function of the wavelength (horizontal axis) and the emission angle θ in air (vertical axis) (a) without gain or scattering; (b) with gain (no scattering); (c) with scattering (no gain); (d) with both gain and scattering. All simulations are made for a gain value below the threshold for lasing.

6. Discussion

First we discuss the comparison between the experimental results of Fig. 2 and the numerical simulations of Fig. 4. The numerical simulations are carried out for a cell that is thinner than the one used in the experiments. The reason is that the calculations become increasingly difficult for thicker cells, because the emission peaks become much narrower, and a higher resolution is needed (both in wavelength and in emission angle) to describe the behavior appropriately. Another difference is that the emission spectrum and the gain coefficients in the simulations are independent of the wavelength. This allows to interpret the effect of gain and scattering. However, we know that the emission and gain spectrum for PM597 have a maximum around 590 nm and therefore the experimental emission in Fig. 2 is higher in this region.

The measurement for low excitation Fig. 2(a) can be compared to the simulation without gain (Fig. 4(a)). In Fig. 4(a) the band around 590 nm is not visible because we assume a white spectrum. The typical angle dependency of the LWE spectrum is similar in both cases. For low excitation, there may also be scattering, but the effect on the emission characteristics is expected to be limited.

The experimental result for high excitation in Fig. 2(c) can be compared to the simulation with gain and scattering of Fig. 4(d). In both cases the effect of scattering is prominent and there is a high intensity of the SWE at 0° which leads to scattering of light with the same wavelength λ*. The vertical line remains visible in the band gap and where the vertical line at 556 nm crosses the angle-dependent LWE curve there is an increased intensity. The values for the wavelengths and angles are slightly different for experiment/simulation, with: λ_{SWE} at 0°: 556 nm/555 nm (= λ*); λ_{LWE} at 0°: 637 nm/642 nm; θ_{SWE} at λ*: 55°/58°(= θ*), but the

Optics EXPRESS

general trend is remarkably similar. Note that in the experiment the vertical (scattering) line at 637 nm has two additional (weaker) maxima at 16° and at 21°. These maxima correspond to secondary reflection peaks where the phase of μ is zero. The value of this angle depends strongly on the thickness of the device and therefore the angles of the additional maxima in the simulation are larger than in the experiment.

Note that in the simulations the emission is calculated below the threshold for lasing. To simulate simultaneous lasing from different peaks, a more sophisticated model that includes mode competition is required. However, the numerical model clearly indicates for which wavelengths and angles the threshold for lasing is approached. It appears that scattering is a good model to explain the coupling between the SWE and LWE modes in the case of ring lasing.

In the simulations the intensity of the LWE emission (Fig. 4(d)) does not depend strongly on the wavelength (except near the SWE). By introducing a wavelength dependency for the emission and gain, it may be possible to explain also the color cone amplified spontaneous emission. This occurs along the section of the LWE that corresponds with the maximum gain in the emission spectrum.

A similar coupling between the SWE at 0° and the LWE (at θ* = 35°) has previously been found experimentally [8,9,20,21]. In one of these papers, the mechanism for coupling has been described as induced fluorescence enhancement [15]. The fact that emission appears at different angles (where strong feed-back is absent) indicates that the mechanism cannot be stimulated emission or amplified spontaneous emission. Therefore, the mechanism of scattering seems the most logical explanation. It is known that light scattering in liquid crystal is induced by director fluctuations and is several orders of magnitude larger than for isotropic fluids [22]. In a liquid crystal cell with thickness of 10 μm, the scattering of transmitted light is expected to be small (order of 1%). However, for light that is generated in the CLC near the wavelength edges, the field is enhanced by multiple reflections, which increases the probability of scattering. Note that scattering does not only explain the coupling between the SWE at 0° and the LWE at 55°, but also the coupling between emissions with different azimuth angles φ. This coupling helps to explain why the observed ring lasing (at 55°) and color cone amplified spontaneous emission (between 40° and 45°) have intensities that are more or less independent of the azimuth angle.

According to the approximate Eq. (1), ring lasing that corresponds to coupling of SWE at 0° and LWE emission at the same wavelength should appear at an angle:

$$\theta^* = \arcsin\sqrt{n_e^2 - n_o^2} \tag{15}$$

For E7 which has high anisotropy, this formula (for n_o = 1.5254 and n_e = 1.7478 at 556 nm according to [18]) yields θ^* = 58°. For the experiments by Lee et al. [9] that are based on ZLI2293 with n_o = 1.50 and n_e = 1.63 (smaller anisotropy) we obtain θ* = 39° This corresponds well with the angle of 35° they have found experimentally.

7. Conclusion

In this work we have measured and simulated the effect of gain and scattering in chiral nematic liquid crystal doped with fluorescent dye molecules. The emission is represented in diagrams that simultaneously show the dependency on the wavelength and on the inclination angle in air. The measurements show that depending on the power density of the incident beam, fluorescence or lasing may be observed. At high intensity different lasing peaks are observed: in the perpendicular direction for $\lambda_{SWE}(0°)$ and for $\lambda_{LWE}(0°)$, and for the angle θ* when $\lambda_{LWE}(\theta^*) = \lambda_{SWE}(0°)$. The numerical simulations show that the combined effect of gain and scattering leads to coupled amplification between the perpendicular emission (at the SWE) and the ring LWE emission at θ*. This is in good agreement with our experimental observations.

Optics EXPRESS

Funding

Research Foundation – Flanders, Fonds Wetenschappelijk Onderzoek (FWO) (PhD fellowship grant of Inge Nys); Ghent University Special Research Fund Bijzonder Onderzoeksfonds (BOF) (PhD fellowship grant for Frederik Van Acker).

References

1. J. H. Lin, P. Y. Chen, and J. J. Wu, "Mode competition of two bandedge lasing from dye doped cholesteric liquid crystal laser," Opt. Express **22**(8), 9932–9941 (2014).
2. H. Coles and S. Morris, "Liquid-crystal lasers," Nat. Photonics **4**(10), 676–685 (2010).
3. J. Ortega, C. L. Folcia, and J. Etxebarria, "Upgrading the Performance of Cholesteric Liquid Crystal Lasers: Improvement Margins and Limitations," Materials (Basel) **11**(1), 5 (2017).
4. V. I. Kopp, B. Fan, H. K. M. Vithana, and A. Z. Genack, "Low-threshold lasing at the edge of a photonic stop band in cholesteric liquid crystals," Opt. Lett. **23**(21), 1707–1709 (1998).
5. J. Schmidtke, W. Stille, H. Finkelmann, and S. T. Kim, "Laser emission in a dye doped cholesteric polymer network," Adv. Mater. **14**(10), 746 (2002).
6. C.-T. Wang, C.-W. Chen, T.-H. Yang, I. Nys, C.-C. Li, T.-H. Lin, K. Neyts, and J. Beeckman, "Electrically assisted bandedge mode selection of photonic crystal lasing in chiral nematic liquid crystals," Appl. Phys. Lett. **112**(4), 043301 (2018).
7. T. Dadalyan, R. Alaverdyan, I. Nys, Z. Ninoyan, O. Willekens, J. Beeckman, and K. Neyts, "Tuning the lasing wavelength of dye-doped chiral nematic liquid crystal by fluid flow," Liq. Cryst. **44**, 372–378 (2017).
8. C. R. Lee, S. H. Lin, H. C. Yeh, T. D. Ji, K. L. Lin, T. S. Mo, C. T. Kuo, K. Y. Lo, S. H. Chang, A. Y. G. Fuh, and S. Y. Huang, "Color cone lasing emission in a dye-doped cholesteric liquid crystal with a single pitch," Opt. Express **17**(15), 12910–12921 (2009).
9. C. R. Lee, S. H. Lin, H. C. Yeh, and T. D. Ji, "Band-tunable color cone lasing emission based on dye-doped cholesteric liquid crystals with various pitches and a pitch gradient," Opt. Express **17**(25), 22616–22623 (2009).
10. C. R. Lee, S. H. Lin, H. S. Ku, J. H. Liu, P. C. Yang, C. Y. Huang, H. C. Yeh, T. D. Ji, and C. H. Lin, "Spatially band-tunable color-cone lasing emission in a dye-doped cholesteric liquid crystal with a photoisomerizable chiral dopant," Opt. Lett. **35**(9), 1398–1400 (2010).
11. S. P. Palto, N. M. Shtykov, B. A. Umanskii, and M. I. Barnik, "Multiwave out-of-normal band-edge lasing in cholesteric liquid crystals," J. Appl. Phys. **112**(1), 013105 (2012).
12. L. Penninck, P. D. Visschere, J. Beeckman, and K. Neyts, "Simulating the Emission Properties of Luminescent Dyes within One-Dimensional Uniaxial Liquid Crystal Microcavities," Mol. Cryst. Liq. Cryst. (Phila. Pa.) **560**(1), 82–92 (2012).
13. L. Penninck, P. De Visschere, J. Beeckman, and K. Neyts, "Dipole radiation within one-dimensional anisotropic microcavities: a simulation method," Opt. Express **19**(19), 18558–18576 (2011).
14. L. Penninck, J. Beeckman, P. De Visschere, and K. Neyts, "Numerical simulation of stimulated emission and lasing in dye doped cholesteric liquid crystal films," J. Appl. Phys. **113**(6), 063106 (2013).
15. S. H. Lin and C. R. Lee, "Novel dye-doped cholesteric liquid crystal cone lasers with various birefringences and associated tunabilities of lasing feature and performance," Opt. Express **19**(19), 18199–18206 (2011).
16. D. Y. K. Ko and J. R. Sambles, "Scattering Matrix-Method for Propagation of Radiation in Stratified Media - Attenuated Total Reflection Studies of Liquid-Crystals," J. Opt. Soc. Am. A **5**(11), 1863–1866 (1988).
17. L. Penninck, J. Beeckman, P. De Visschere, and K. Neyts, "Light emission from dye-doped cholesteric liquid crystals at oblique angles: Simulation and experiment," Phys. Rev. E Stat. Nonlin. Soft Matter Phys. **85**(4 Pt 1), 041702 (2012).
18. J. Li, C. H. Wen, S. Gauza, R. B. Lu, and S. T. Wu, "Refractive Indices of Liquid Crystals for Display Applications," J. Disp. Technol. **1**(1), 51–61 (2005).
19. J. Etxebarria, J. Ortega, C. L. Folcia, G. Sanz-Enguita, and I. Aramburu, "Thermally induced light-scattering effects as responsible for the degradation of cholesteric liquid crystal lasers," Opt. Lett. **40**(7), 1262–1265 (2015).
20. C. R. Lee, S. H. Lin, J. D. Lin, T. S. Mo, C. T. Kuo, and S. Y. Huang, "Unique spatial continuously tunable cone laser based on a dye-doped cholesteric liquid crystal with a birefringence gradient," Appl. Phys. B **109**(1), 159–163 (2012).
21. C. R. Lee, S. H. Lin, H. S. Ku, J. H. Liu, P. C. Yang, C. Y. Huang, H. C. Yeh, and T. D. Ji, "Optically band-tunable color cone lasing emission in a dye-doped cholesteric liquid crystal with a photoisomerizable chiral dopant," Appl. Phys. Lett. **96**(11), 111105 (2010).
22. S. T. Wu and K. C. Lim, "Absorption and Scattering Measurements of Nematic Liquid Crystals," Appl. Opt. **26**(9), 1722–1727 (1987).